

# Generation of docking ligands to F13L mutations isolated in MonkeyPoxVirus-infected patients resistant to Tecovirimat-treatment

short title: monkeypox co-evolutionary docking

Coll, J.

Department of Biotechnology. Centro Nacional INIA-CSIC. Madrid, Spain.

\* Corresponding author

Email: juliocollm@gmail.com (JC)

Julio Coll, orcid: 0000-0001-8496-3493

## Abstract

Alternative drugs are actively searched because of the recent identification of F13L mutations in MonkeyPox Virus (MPXV)-infected patients with resistances to Tecovirimat-treatment. Aiming to help on these searches, computational strategies to generate rather than to screen for new drug-like ligand candidates were explored here. Targeting F13L-mutant representative models, thousands of fitted-children ligands were predicted by i) co-evolutions from the Tecovirimat parent molecule, and ii) F13L-mutant models limited by pooling the most abundant mutations isolated from Tecovirimat-treated patients. Children-fitting F13L-mutant docking-cavities predicted novel scaffolds, nanoMolar affinities, high specificities, absence of known toxicities and conservation of their parent-docking cavities. Despite their limitations, such proved-on-concept similar strategies might be fine-tuned to computational explore for new drugs the most prevalent Tecovirimat-resistance mutants.

Keywords: co-evolutionary docking; Tecovirimat-resistant mutations; ST-246; monkeypox virus; MPXV; F13L

## Introduction

This computational work explored new ligand alternatives to Tecovirimat (ST-246 or TPOXX, here ST246) which maintained their docking to ST246-resistant mutants arising during the 2022 MPOX outbreak caused by the **MonkeyPoxVirus** (MPXV). The ST246 reference FDA-approved inhibitor for vaccinia poxvirus<sup>2</sup>, was used here as the parent molecule to derive children by co-evolutions. Randomly generated children were selected by best fitting to F13L alphafold models including pooled mutations associated with ST246-resistance. For that, co-evolution was used following the **DataWarrior Build Evolutionary Library** algorithms (DW-BEL) algorithms<sup>2-5</sup>. DW-BEL mimicked natural co-evolution by randomly generating tens of thousands of ST246 children, discarding low fitting and saving the best F13L-fitted children<sup>1</sup>, rather than screening preexisting compound libraries. By incorporating Toxicity Risk assessment<sup>1</sup> and increasing computer memories during co-evolution, thousands of non-toxic children were generated that predicted drug-like properties, nanoMolar affinities, and higher specificities while conserving their F13L mutant docking cavities.

The wild type F13L (p37) are the most abundant of the poxviral peripheral membrane proteins. Coding for 37 kDa (372 amino acids)<sup>2,3</sup>, F13L contain two residues that can be palmitoylated (I<sup>85</sup>CC), two phospholipase-like motifs (~<sup>121</sup>xxxxDD and near-canonical <sup>312</sup>NxKxxxD)<sup>4-7</sup>, and one mutation sensitive motif (<sup>253</sup>YW) to interact with cellular TIP47<sup>8</sup>. F13L co-localizes<sup>12,27</sup> with B5R (B6R orthologous in MPXV)<sup>9-11</sup>, which could be also palmitoylated (<sup>301C</sup><sup>303C</sup>)<sup>12</sup> and belong to transmembrane anchored glycoproteins of 42 kDa (317 amino acids)<sup>13</sup>. B5R(B6R) contains an extracellular domain, a transmembrane  $\alpha$ -helix and a short cytoplasmic tail<sup>14,15</sup>. F13L and B5R proteins are both required for vaccinia poxviruses to be released from their infected cells<sup>16</sup>. F13L and/or B5R deletions caused inhibition of membrane wrapping, fewer extracellular viral particles and attenuation of the resulting poxviruses<sup>15,16-19</sup>.

The so called here ST246, was chosen to target MPXV because it is a FDA-approved F13L strong-ligand for poxviruses. ST246 is active at low nanoMolar concentrations in vaccinia and also inhibits MPXV infections<sup>20-23,29</sup>. Thus, ST246 and several analogues have been recently recommended to inhibit MPXV with an estimated EC<sub>50</sub> of ~150 nM<sup>17-20</sup>. ST246 is a small molecule containing a complexing structure, inhibiting poxviral membrane wrapping and replication of most poxviruses including vaccinia, MPXV, variola, smallpox, cowpox, camel, and others<sup>21</sup>. However, despite its reported inhibitory activities, F13L-ST246 complexes have not been crystallographically reported yet. With respect to its mechanism of inhibition, it was demonstrated that ST246 changes the intracellular membrane co-localizations of vaccinia F13L (from membrane to cytoplasm) and B5R (disaggregation from Golgi to vesicles)<sup>22</sup> and reduces the immunoprecipitation of F13L-B5R complexes<sup>9</sup>. However, no F13L-B5R(B6R) complex structures have been yet reported.

F13L surface shallow grooves have been proposed as F13L-ST246 docking cavities using different computational docking efforts<sup>17,23-25</sup>. The most recent docking study predicted 19 MPXV F13L amino acid residues for ST246 contacts in the most probable binding site, validating their hypothetical interactions by detailed molecular dynamic-docking studies<sup>26</sup> (**Table S3, yellow left**). Although the mechanisms of inhibition are unknown, ST246 has been proposed to conformationally disturb the near-canonical phospholipase motif of F13L to interfere with its activity<sup>24</sup>. Alternatively, ST246 may still fit other F13L binding cavities to block yet-unknown functions, including the possible dissociation of F13L complexes with other proteins (i.e. poxviral B5R/B6R).

ST246-resistant mutations generated by cell culture *in vitro* identified unique targets at F13L amino acid residues conserved among several poxviruses<sup>3</sup>.

<sup>4</sup>. Some of those resistant mutations were located toward its carboxy-terminal domain<sup>28,29,32</sup>. Most recently, some of those earlier reported poxvirus mutations were confirmed while other were reported for the first time in MPXV patients resistant to ST246-treatment (**Table S2 and Figure 1<sup>26-28</sup>**). These recent results suggested that at least in 1-5 % of the MPXV patients, the resistance mutations arise after ST246 treatment, specially in immunocompromised patients where those percentages could be even higher<sup>29</sup>. Therefore, alternative drugs are needed, since no other potent inhibitors targeting ST246-resistant poxviruses have been yet reported<sup>26-28</sup>, despite many research efforts<sup>18</sup>.

We report here some limited first attempts to generate large amounts of alternative ligands to ST246 by DW-BEL co-evolution in F13L pooled mutants. The successful targeting of DW-BEL to hypothetical ST246-resistant mutant cavities by co-evolution and blind-docking, required both high computer memories to apply toxicity risk assessments and specificity (molecular weight and hydrophobicity) to control their tendencies to increase<sup>6,7,8-11</sup>. The accuracy of the predictions was improved by preserving 2D geometries to seek DW-BEL consensus with **AutoDockVina** (ADV), recently identified as one of the most successful docking predictors<sup>31</sup>.

The conservation of similar F13L docking cavities in children ligands to the F13L pooled mutants than to those at the initial ST246 parent, could be interpreted as a favorable prediction sign of their possible inhibitory activities. However, predictions remain highly hypothetical because the absence of crystallographic structures, limitation to pooling the most abundant resistant mutations and/or experimental confirmations. Nevertheless, perhaps similar strategies could be applied once the prevalence of ST246-resistant MPXV mutants would be more studied.

## Computational Methods

### Modeling of the F13L from the MPXV 2022 strain with ST246-resistant mutations

The amino acid sequences corresponding to the F13L from the 2022 multinational outbreak of MPXV infection corresponding to isolated clade IIb lineage B.1 (containing the E353K mutation)<sup>23</sup>, was downloaded from GenBank URK20480. The F13L amino acid sequence was alphafold modeled (F13L0) (<https://colab.research.google.com/github/sokrypton/ColabFold/blob/main/AlphaFold2.ipynb>), obtaining a **Root Mean Square Deviation** (RMSD) of 9.6 Å with the crystallographic model of the phospholipase D of *Streptomyces sp* (ID 1v0y) at <https://www.rcsb.org/structure/><sup>4</sup>.

The F13L coding for pools of the most abundant ST246-resistant mutations<sup>23</sup> (**Table S2 and Figure 1 red solid circles**) were introduced into their amino acid sequences before being uploaded to Alphafold. The five alphafold models obtained in each case predicted minimal RMSD of ~ 0.2 Å differences among them. Therefore, models number 1 were selected for the computational studies. The new mutants contained a pool of the common E353K and the most abundant ST246-resistant mutations as follows, mutant **F13L1** (mutations E353K+N267D+ A288P+ A290V+ D294V+ A295E+ I372N) and mutant **F13L2** (mutations E353K+ N267deleted+ A288P+ A290V+ D294V+ A295E+ I372N). The F13L2 alphafold model required one additional "clean geometry" step by Discovery Studio, to relax their predicted 3D structure as required for DW-BEL, most probably due to the inclusion of the N267 deletion.

The PubChem (<https://pubmed.ncbi.nlm.nih.gov/>) 2D and 3D sdf files of ST246, Tecovirimat, ST-246 or TPOXX (4-trifluoromethyl-N-(3,3a,4,4a,5,5a,6,6a-octahydro-1,3-dioxo-4,6-ethenocycloprop[*f*] isoidol-2(1H)-yl)-

benzamide)<sup>21</sup> and Ciclofovir, IMCBH (Nisonicotinoyl-N,-3-methyl-4-chlorobenzoylhydrazinc)<sup>30</sup>, were employed as F13L poxviral reference ligands.

### The DataWarrior "Build Evolutionary Library"

The DataWarrior (DW) updated program was downloaded (<https://openmolecules.org/datawarrior/download.html>) following the Windows details (dw550win.zip for Windows), as described before<sup>1, 31</sup>.

The DW/Chemistry /Dock structures into protein cavity and /Build Evolutionary Library (DW-BEL) were loaded to Load Protein Cavity From PDB-File<sup>1</sup>. Briefly, the corresponding \*.pdb docked files provided target docking cavities predicted by previous ADV blind-docking and \*.sdf files provided the 2D structure of parent for co-evolutions. Preference criteria values and their weights for DW-BEL were as follows: minimal DW docking-scores (weight 4), molecular weight <= 600 g/mol, LogP <= 4 (weight 1) and Toxicity risk <=1 (weight 4).

To best preserve 2D geometries of the generated children, the DW mmff94s+ force-field minimization algorithm<sup>32</sup> was critical<sup>31</sup>. DW docking ranked the children by unit-less relative negative values (the more negative, the higher affinities). From each parent, 3 consecutive runs generated thousands of unique best-fitting children molecules<sup>1</sup>. The raw children \*.dwar files permanently saved docking-scores, molecular weights, cLogP hydrophobicities, and cavity-children docked images. The \*.dwar files labeled with their number of ligands and experiment name were filtered using a DW macro to exclude hundreds of children with remaining toxicities (Mutagenesis, Tumorigenicity, Reproductive interference, Irritant, and Nasty functions)<sup>33</sup>.

To accurately prepare the children for external programs (i.e., PyMol, ADV docking), the following DW /File/Save Special/SD-File.... optimized options were selected to preserve 2D geometries of conformers when saving \*.sdf files: Structure column: Docked Protonation State, SD-file version: Version 3, Atom coordinates: Docking pose, □option checked: checked Cavity & Natural Ligand, Compound name column: ID. These \*.sdf files optimally uploaded to PyMol for visualization (using its split\_states command<sup>31</sup>) and/or to PyRx/Obabel-ADV for minimization and \*.pdbqt file generation and docking.

### The AutoDockVina docking program

The AutoDockVina (ADV) program written in Python vs3.8 included into the PyRx-098/PyRx-1.0 package<sup>46</sup> (<https://pyrx.sourceforge.io/>), and home-modified to handle large number of ligands, was used as described before. As recently reported, ADV was the best binding predictor for 428 protein-ligand complexes ( $\pm 2 \text{ \AA}$ ), among 9 other docking programs, including 2 new amino acid sequence-smile-only algorithms, with the highest 52.3 % of success prediction rate<sup>34</sup>. ADV was employed here to explore alternative docking cavities than those identified by DW, to compare ADV affinities with DW docking-scores, to estimate relative docking in ~nanoMolar (nM) affinities and to generate detailed PyMol protein / children 3D images<sup>31, 35-37</sup>. Briefly, Obabel minimization and \*.pdbqt file conversion of F13L proteins and children ligands<sup>38</sup> were generated by employing the mmff94s (Merck) force-field (most similar to the DW-BEL mmff94s+). Children ligands were supplied to Obabel-ADV as DW-BEL generated \*.sdf files, saved as mentioned above to preserve their 2D geometries. Only the highest affinity conformers were analyzed in this work. Estimates of ADV ~ docking-scores in Kcal/mol<sup>39, 36, 40, 41</sup>, were converted to ~ nM affinities by the formula,  $10^{9 \cdot (-\text{exp}(\text{Kcal/mol} / 0.592))}$ . A blind-docking grid of 45x45x45 Å centered to PyMol / centerofmass, surrounding the whole F13L models were employed.

### Computational software and hardware

In this work, 128 Gb of computer RAM memory, and options for saving \*.sdf file for optimal 2D conservation, were introduced. Details provided on Table 1 were as described before<sup>1</sup> and included here for convenience.

Table 1

Software and hardware for computational manipulations

name	vs	Main use	url
DataWarrior (DW)	Updated 5.5.0 Windows/Linux	Evolutionary docking <sup>34</sup> Docking to protein cavity Mmff94s+ force-field 2D conservation *.sdf files NTN Toxicity/Nastic macro	<a href="https://openmolecules.org/datawarrior/download.html">https://openmolecules.org/datawarrior/download.html</a> <a href="https://cheminfo.github.io/openchemlib-s/classes/ForceField/MMFF94.html">https://cheminfo.github.io/openchemlib-s/classes/ForceField/MMFF94.html</a> <a href="https://github.com/cheminfo/openchemlib-js/blob/8868a0/types.d.ts#L3333">https://github.com/cheminfo/openchemlib-js/blob/8868a0/types.d.ts#L3333</a> <a href="https://openmolecules.org/forum/index.php?1=msq&amp;th=662&amp;start=0&amp;">https://openmolecules.org/forum/index.php?1=msq&amp;th=662&amp;start=0&amp;</a> <a href="https://openmolecules.org/forum/index.php?1=msq&amp;th=632&amp;start=0&amp;">https://openmolecules.org/forum/index.php?1=msq&amp;th=632&amp;start=0&amp;</a>
Babel & AutoDockVina	Home-adapted PyRx 0.98/1.0	Force-field minimization & 2D-reliable docking	<a href="https://pyrx.sourceforge.io/">https://pyrx.sourceforge.io/</a>
MolSoft	3.9 Win64bit	Manipulation of *.sdf files	<a href="https://www.molsoft.com/download.html">https://www.molsoft.com/download.html</a>
PyMol 2023	2.5.7.	Visualization of molecules 3D alignment	<a href="https://www.pymol.org/">https://www.pymol.org/</a>
Discovery Studio	21.1.1.0.20298	Visualization of molecules Structure/clean geometry	<a href="https://discover.3ds.com/discovery-studio-visualizer-download">https://discover.3ds.com/discovery-studio-visualizer-download</a>
OriginPro	2022	Mathematical, statistical calculations and Figures	<a href="https://www.originlab.com/">https://www.originlab.com/</a>
LigPlus+	2.2.8.	Amino acid targeted by docked ligands around 4 Å	<a href="https://www.ebi.ac.uk/thornton-n/software/LigPlus/appliance.html">https://www.ebi.ac.uk/thornton-n/software/LigPlus/appliance.html</a>
DW / Chem-Space	Oct26th 2023	Commercially available chemical analogues	<a href="https://chem-space.com/">https://chem-space.com/</a>
AMD Ryzen i9 computer	4 DDR4 x 32 Gb memory	47 CPU Computational hardware	<a href="https://www.pcspecialist.es/">https://www.pcspecialist.es/</a>

## Results

### F13L models

Early for a complete scenario of MPXV ST246-resistance mutants, studies of the 2022 outbreak mapped F13L amino acid mutations of ST246-treated 26 patients<sup>23, 27, 28</sup>. This work constitute the largest number of ST246-resistant MPXV isolates from humans reported to date<sup>23, 27, 28</sup>. All those 2022 MPXV isolates belonged to the clade IIb lineage B.1, which codes for the E353K mutation (unrelated to ST246 resistance), compared to the reference MPXV strain isolated in 200323. Because it is not yet clear which of the individual- or multi-mutation mutant isolates could be related to ST246 resistance or be necessary for mutant poxviral survival, models included the most abundant mutations appearing in the 26 patients.

All the F13L described mutations included i) early reported poxvirus mutations generated by *in vitro* selection<sup>24</sup>, ii) mutations found recently by screening healthy patients<sup>23, 27, 28</sup> and iii) mutations isolated from ST246-treated patients<sup>23, 27, 28</sup> (Table S2). Most of these mutations mapped between the ~ 200 to 300 amino acid F13L residues, before the near-canonical phospholipase-like motif (Figure 1, green circles, red circles). In contrast, E353K (unrelated to ST246-resistance) and I372N, mapped after the phospholipase motif. This mutational gap (Figure 1 yellow vertical line), could be explained to preserve the poxviral requirement for phospholipase activity.

Among all single F13L mutations, those showing the highest EC<sub>50</sub> > 500 μM ST246-resistance phenotypes corresponded to multiple mutations (Figure 1, red solid spheres), suggesting that several single mutations might be necessary to confer the highest ST246-resistances. Compared to the MPXV reference strain clade IIa (2003) with a ST246 susceptibility of EC<sub>50</sub> = 17.5 nM (published data from Table 1 of Smith et al<sup>23, 27, 28</sup>), higher EC<sub>50</sub> resistances, suggested to the authors that all these single mutations were developed during human infection ST246-treatments, specially those isolated from immuno compromised patients.

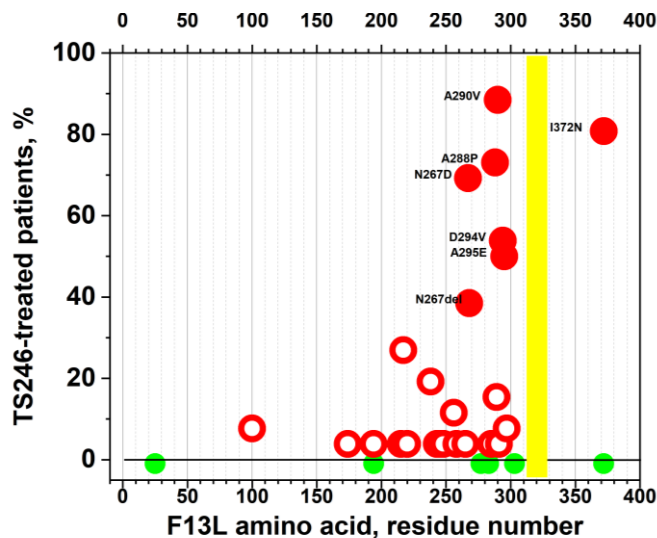


Figure 1

Single mutated amino acids in F13L ST246-treated patients and *in vitro* isolates

Single mutations from single- or multi-mutant isolates were counted in 26 patient isolates (Table S2)<sup>23</sup>. Their percentages were calculated by the formula,  $100 \cdot \text{number of single mutations} / 26$  (data from Table 1<sup>28</sup>). All the MPXV 26 isolates from the 2022 outbreak at Los Angeles USA coded for E353 and therefore these mutations were unrelated to ST246-resistance<sup>23, 27, 28</sup>. Yellow vertical rectangle, mapped near-canonical phospholipase-like motif (<sup>312</sup>NxKxxxX)<sup>4, 5</sup>. Green circles, previously reported F13L poxvirus *in vitro* mutations. Red circles, single mutations identified from 26 patient isolates assayed for ST246-resistance. Red solid circles, mutations included into the F13L1 and F13L2 mutant models. Selected because they showed the highest i) percentages in the 26 patient isolates and ii) resistances > 500 μM of ST246<sup>28</sup>. Their single amino acid mutations were labeled to their left (wild-type amino acid-position number-single mutation). Green solid circles, mutations isolated *in vitro* by cell co-culture of several poxvirus with ST246<sup>24</sup>.

To explore for possible new ligands to F13L-mutants by DW-BEL co-evolution, representative F13L mutant models were included into the amino acid sequences before being modelled at Alphafold. The reference 2003 MPXV strain (F13L-1), the common 2022 E353K clade IIb mutation of the 2022 outbreak (F13L0) and the representative pooled mutants coding for the most abundant and highest EC<sub>50</sub> ST246-resistant mutations (F13L1 and F13L2) (Figure 1, labelled red solid circles) were all Alphafold modelled.

Because the main objective of this work was to test prove-of-concept computational strategies rather than to develop a practical application, a minimal number of two representative F13L mutant models containing the most abundant and higher resistance mutations were selected for these early preliminary studies. Two models were required because N267D / N267deleted mutations exclude each

other, and should not be discarded due to their high frequencies and to the high structural impact of the N267 deletion. In addition to the single mutations, the common background mutation E353K was included also. Therefore, the artificially designed pooled-mutant models were, **F13L1** (coding for E353K + N267D + A288P + A290V + D294V + A295E + I372N) and **F13L2** (coding for E353K + N267deleted + A288P + A290V + D294V + A295E + I372N).

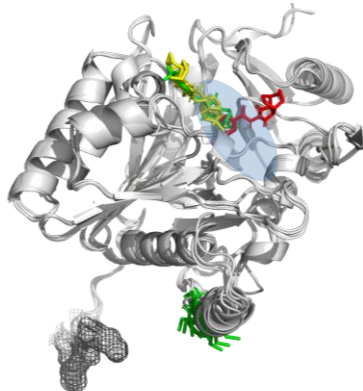


**Figure 2**  
ST246-docked to AlphaFold modeled F13Ls  
The ST246 was blind-docked by ADV to F13L-1 (reference strain of 2003), F13L0 (common E353K mutation of the 2022 clade), and ST246-resistant pooled single mutations F13L1 and F13L2 coding for most abundant single mutations isolated in 2022. All the 4 individual images were merged in PyMol.

**Gray cartoons**, merged F13L-1, F13L0, F13L1 and F13L2 AlphaFold modeled amino acid carbon alpha (CA) backbones.  
**Yellow sticks up**, ST246-docked to F13L-1 and to F13L0.  
**Green sticks up**, ST246-docked to F13L1.  
**Red sticks up**, ST246-docked to F13L2.  
**Green sticks down**, palmytoil sites at <sup>185</sup>CC  
**Black mesh down**, amino terminal <sup>1</sup>Met  
**Blue background ellipse**, ~ near-canonical phospholipase-like <sup>312</sup>NxKxxxxD motif and required <sup>334</sup>H<sup>338</sup>H, mapping behind the docked ST246 cavities.

#### ADV blind-docking of ST246 to F13L wild-type and representative mutants

An automatically centered 45x45x45 Å grid, similar to the one proposed for the F13L MPXV strain isolated in 2007<sup>25</sup>, was selected for this work, after testing and evaluating different grid sizes (Table S1). Such wide grid surrounded most of the F13L molecules (blind-docking) in all the F13L models including those coding for the single pooled mutations.

ADV blind-docking results predicted that the ST246-docked F13L-1, F13L0 and F13L1 at similar docking cavities (Figure 2, yellow and green sticks), while ST246-docked F13L2 to a nearby different cavity (Figure 2, red sticks). It seems most reasonable that ST-246 docking to F13L2 were more affected than any of the F13L models because it coded for the N267 deletion.

The ST246-docking to F13L0, predicted similar amino acids at 4 Å distance than those reported before<sup>25</sup> (Table S3, yellow left columns). The wide blind-docking grid, allowed the exploration of any alternative docking cavities, while predicted the highest affinities for ST246 and IMCBH<sup>42</sup> (Table S1). The near canonical phospholipase-like motif (<sup>312</sup>NxKxxxxD)<sup>4, 5</sup>, their probable <sup>334</sup>H<sup>338</sup>H requirements for phospholipase activity, and the E353K mutation present in all isolates of the MPXV 2022 outbreak, mapped behind ST246 (Figure 1, Blue background ellipse, Table S3, yellow columns).

#### Best-fitted children to F13L cavities

Because whole ST246-parent molecules predicted children with higher affinities and lower toxicities than using their fragments as parents (data not shown), the whole ST246 was chosen for further work. Because targeting criteria with molecular weight preferences <280, <300, <400, <500 or <550 g/mol, did not greatly increased their children affinities, molecular weights < 600 g/mol were targeted. Targeting molecular weights > 600 g/mol were discarded because of the risk to increase both unespecificity and computer memory demands. To target children with < 600 g/mol, the computer memories were increased from 60 to 120 Gb to avoid program crashes, improve the co-evolution speed and increase the number of fitted-children (Figure S1, up). Such high memories may be required to keep track of the tens of thousands of raw children generated during co-evolutions and to select among them thousands of unique fitted-children<sup>1</sup>. The progressive reduction of docking-scores, visualized the increase affinities (lower binding-scores) during each of 3 consecutive runs (Figure S1, down).

#### Representative top-children fitting F13L1 and F13L2 pooled mutants

The comparison between DW-BEL and ADV predicted different profiles for ST246-derivatives targeting F13L1 (green) and F13L2 (red) (Figure 3). Most of those children predicted higher affinities than ST246 (Figure 3 solid circles in green and red). However, because of their very different algorithms, docking-score calculations and targeted cavities/grids, the DW-BEL docking-scores did not exactly correlated with ADV affinities (Figure 3).

F13L1 top-children were selected using a home-made python script (available upon request) which predicted DW-BEL docking-scores < - 85 and ADV affinities < -11 nM. All 32 top-children targeted similar F13L1 docking-cavities (Figure 4 up) than ST246 (Figure 2, green). The top-children consisted in two different scaffolds of 6 rings with different atom extensions, 2-3 Nitrogen atoms and 6 Oxygen atoms (Figure 5, 12326 and 8181, and Table 2).

F13L2-targeted children were selected by predicting DW-BEL docking-scores < - 90 and ADV affinities < -10 nM (as described above). Some of the 36

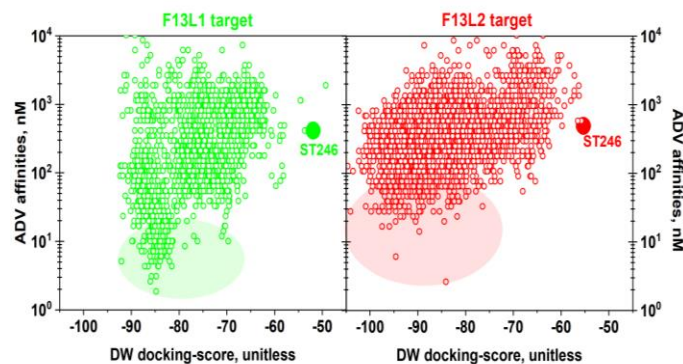


**Figure 3**  
ADV versus DW-BEL of ST246 co-evolved children targeting F13L1 or F13L2  
The corresponding F13L1- or F13L2-ST246 docked cavities were targeted by DW-BEL to generate children from the ST246 parent. Then, the DW-BEL children were blind-docked by ADV using a 45x45x45 Å grid to identify possible alternative cavities and quantify their affinities in ~ nM.  
**Green open circles**, F13L1. **Solid green circle**, ST246. **Green oval background**, F13L1 top-children.  
**Red open circles**, F13L2. **Solid red circle**, ST246. **Red oval background**, F13L2 top-children.

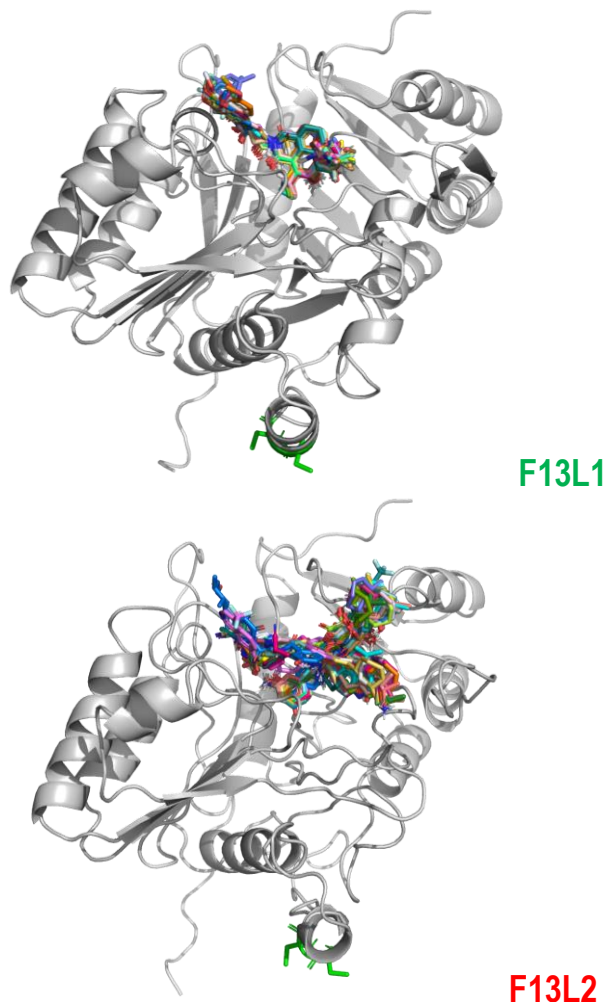


**Figure 4**  
Mapping of top-children derived from ST246 targeting F13L1 and F13L2 docking-cavities  
Gray cartoons, carbon backbone of F13L1 and F13L2 as in Figure 2.  
**Green sticks in F13L α-helix** Dipalmitoylated 185 and 186 Cysteines of F13L  
**Multicolor sticks**, 32 or 36 top-children docked to F13L1 or F13L2, respectively.

top-children targeted similar docking-cavities (Figure 4 down) than ST246 in F13L2 (Figure 2, red), while other targeted similar docking-cavities than those targeted by ST246 in F13L1 (Figure 2, green). The top-children consisted in 3 branches extended from a central carbon (Figure 5, 35702 and 34853) with two different scaffolds with different atom extensions, 3 Nitrogen atoms and 6-7 Oxygens (Table 2). More chemical and docking details of additional top-children could be obtained from the author upon request.

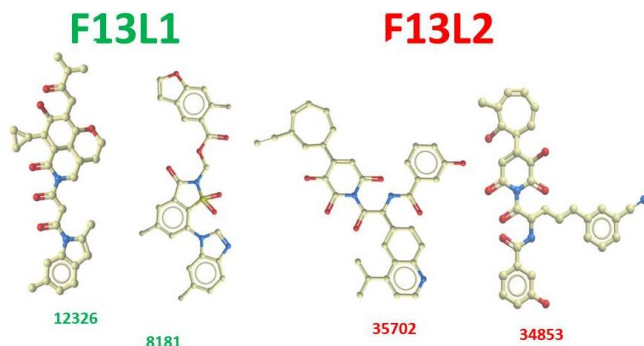


Figure 5  
2D structures of representative scaffolds of top-children targeting F13L1 or F13L2

Table 2  
Properties of representative scaffold of the top-children

Target: Children	DW-BEL, unitless	ADV, nM	Target sites	MW, g/mol	logP	Chemical formula
<b>F13L1:</b>						
12326	-84.8	1.8	X	546	3.5	C32H38N2O6
8181	-81.5	4.3	X	527	4.0	C24H16F3N3O6S
<b>F13L2:</b>						
35702	-94.6	6.0		591	3.5	C35H35N3O6
34853	-95.6	16.7	X	571	2.8	C32H33N3O7

X targeted sites, mapped to the F13L1-ST246 docking cavity (Figure 2, yellow green sticks)  
Unlabelled targeted sites, mapped to the F13L2-ST246 docking cavity (Figure 2, red sticks)

The identification of the F13L1 and F13L2 amino acids surrounding their docked complexes with top-children confirmed the visualized differences among the representative top-children scaffolds (Table S3). Previously unreported, the docking to the F13L1 and F13L2 mutants containing the pooled mutations isolated in ST246-resistant patients, identified some new possible targeted amino acids, compared to previous ST246 studies. Nevertheless, there were many coincidences with some of the amino acids previously reported to be targeted by ST246 docked to the MPXV F13L isolated in 2007 (353E)<sup>25</sup>. For instance, the new top-children targeted amino acids 312N, and 334H 338H located at the near canonical phospholipase-like motif and their Histidine putative requirements, some with Hydrogen bonds (Table S3, red H). Additionally, one of the top-children (35702), predicted Hydrogen bonds to 283D, one amino acid mutated in MPXV and previously isolated by *in vitro* resistance to both ST246 and IMCBH<sup>24</sup>.

## Discussion

These drug-like predictions are limited in their possible applications because i) the small number of available mutations isolated from ST246-resistant patients, ii) the mutant approach followed by pooling the most abundant mutations, and iii) the lack of F13L crystallographic models. Nevertheless, the proposed strategy might be valid for future work when more mutations would be available for further analysis aiming to predict putative ST246-drug alternatives. The recent MPXV outbreak identifying F13L mutations appearing on ST246-resistant immunocompromised human patients, strongly suggested such needs for alternative drugs.

In this preliminary work, we targeted AlphaFold-predicted F13L artificially constructed mutants by pooling most abundant mutations to offer a prove-of-concept of simplify DW-BEL co-evolutions. The first attempts to co-evolve ST246-derived ligands were unsuccessful due to the shallow grooves targeted by ST246 at the F13L surfaces. Apparently, such targets were not capable to generate appropriated cavities for docking even when increasing computer memories and co-evolution runs. After numerous trial-and-error efforts, an alternative strategy was developed. Such strategy mainly consisted in: i) Including highly specific non-toxic filtering during the co-evolution together with higher computer memories, ii) Improving 2D conservation exchanges between DW-BEL / ADV programs by using mmmf94s+ force-field minimizations, and iii) Exploring alternative F13L cavity possibilities by ADV wider blind-docking.

Pending on crystallographic F13L structures, several docking cavities were identified as possible new binding targeting candidates. Furthermore, to complicate F13L docking interpretations, different binding cavities may co-exist or be exchanged by mutations during one MPXV human outbreak even in the same patient. Because of these docking-cavity uncertainties, we also explored some of most recent machine-learning new algorithms using transformers<sup>78, 91, 43-45</sup> that rely only on protein amino acid sequences<sup>46, 47</sup>. Among all that were tested, the Highlights on Target Sequences (HoTS), was one of the most reproducible and successful method to predict binding cavities<sup>91</sup> when applied to F13L (data not shown). Trained with only 232 protein-ligand complexes, HoTS claimed a

successful prediction of ~66 % of binding regions on not-seen-before protein sequences<sup>91, 48</sup>, despite its limitations due to the small numbers of pairs for model training<sup>49</sup>. In our hands, HoTS predicted some of the F13L docking-cavities described before and here (data not shown). However, HoTS was very slow when compared to the speed at which hundreds of ligand children were generated by DW-BEL co-evolution. It appears that sequence-only docking methods would require more development efforts<sup>49, 50</sup>.

Many of the amino acids predicting contacts with top-children confirmed those already identified by previous ST246 docking<sup>25</sup>, including those amino acids surrounding the F13L near canonical phospholipase-like motif and those nearby their Histidines apparently required for activities<sup>4</sup> (334H, 338H), suggesting that those sites may constitute another unexplored target for the future.

Apart from the highly hypothetical F13L1 and F13L2 mutant models including the most abundant mutations, other limitations arise. For instance, the use of fixed rather than dynamic docking-cavities, absence of water interactions, or the always incomplete exploration of the vast chemotype/chemical space<sup>38-39</sup>. Additionally, other docking cavities remain to be further explored, such as those known interactions with other proteins like B6R-poxvirus, and/or TIP47-host proteins.

Some of the most remarkable results on MPXV F13L artificially pooled-mutation mutants was the speed and high numbers of unique nanoMolar affinities generated fitting those models. Many different co-evolution trajectories were identified when providing high computer memories and/or more runs. However, only chemical synthesis (perhaps from Chem-Space analogs) followed by experimental tests, could confirm these predictions to inhibit MPXV isolates from ST246-resistant patients. Some of these ideas may help others to explore alternative ligands to complement the effectiveness of the ST246 drug.

## Supporting Information

Table S1  
ST246 and IMCBH binding and preliminary docking to F13L

method	pox target	F13L model	Grid center, Å			Grid size, Å	ST246 ~ nM	IMCBH ~ nM	reference
			X	Y	Z				
EC50	VACV	Binding	---	---	---	---	6	65000	<sup>42</sup>
QVina	MPXV	afold*	?	?	?	?	820	?	<sup>23</sup>
DiscoveryStudio	MPXV	afold**	-6.2	-2.4	-8.6	8.9 sphere	15	?	<sup>25</sup>
ADV	MPXV	afold*	-6.2	-2.4	-8.6	8.9 sphere	820	?	<sup>17</sup>
ADV	VACV	afold**	-0.2	0.4	1.4	45x45x45	46	4400	selected
ADV	VACV	afold**	-0.2	0.4	1.4	60x60x60	50	1600	this work
ArgusLab	VACV	Swiss*	?	?	?	?	?	?	<sup>24</sup>
ArgusLab	VACV	afold*	-3.0	-3.0	0.9	25x25x25	6180	690	this work
ADV	VACV	afold*	-3.0	-3.0	0.9	25x25x25	6180	35600	this work

\* , grid center defined by ST246<sup>6</sup> and IMCBH<sup>4</sup> mutations. \*\*, grid center automatically selected by LibDock (DiscoveryStudio)<sup>25</sup> or ADV<sup>15</sup> and this work. EC<sub>50</sub> , *in vitro* binding of ST246 and IMCBH<sup>4</sup> nM, affinities calculated from Kcal/mol of ADV docking-scores by the formula, nM=10<sup>3</sup>·(exp(Kcal/mol/0.592)). QVina, QuickVina. ADV, AutoDockVina. VACV, VACcinia Virus. MPXV, MonkeyPox Virus. **Yellow background**, grids selected here

Table S2  
F13L mutations in 26 patients treated with ST246 (data modified from Table 1 from Smith et al 2023<sup>28</sup>)

Mutations	Isolation	Number isolates	Reference
F25V	CMLV	-	24
D100N	patients	2	28
K174N	patient	1	28
H194N	patient+MPXV	1	24, 28
S215F	patient	1	28
D217N	patients	7	28
T220A	recent	?	27
H238Q	patients	5	27, 28
P243S	patient	1	27, 28
T245I	patient	1	27, 28
D248N	patient	1	28
D256N	patients	3	28
Y258C	patient	1	28
A265D	recent	-	27
N267D	patients	18	18, 27, 28
N267deleted	patients	10	18, 27, 28
G277C	VACV,CMLV,MPXV	-	24, 42
D283Y	patient +MPXV	1	24, 28
I285H	patient	1	28
A288P	patients	19	27, 28
T289A	patients	4	27, 28
A290V	patients+VACV patient	23	18, 27, 28
R291K	patient	1	28
D294V	patients	14	27, 28
A295E	patients	13	28
L297inserted	patients	2	28
D301deleted	patient	?	28
S369L	patient	?	28
SVK303-305	MPXV	-	24
E353K	2022 outbreak	26	28
I372N	patient +VACV,CMLV	21	24, 27, 28

**Blue background** Mutations from either patients or *in vitro* ST246-resistant  
**Light blue background**, recently detected, not yet assayed for ST246 resistance  
**Strong blue background**, The 26 MPXV isolates belonged to clade IIb lineage B.1 coding for the E353K mutation compared to the previous reference strain.  
**Reddish background**, most abundant mutations mapped alone or together  
VACV, *in vitro* isolated VACcinia Virus resistance mutations  
MPXV, *in vitro* isolated MonkeyPox Virus resistance mutations  
CMLV, *in vitro* isolated CaMeL Virus resistance mutations

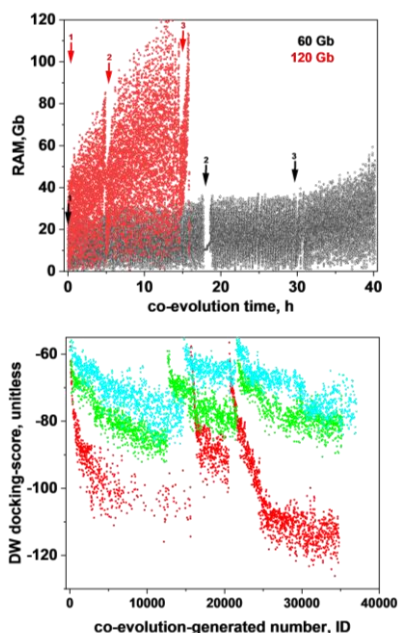


Figure S1

Timing of two memory demands during DW-BEL co-evolutions (Up), and children docking-scores versus their co-evolution-generated ID number (Down)

The DW-BEL co-evolution randomly generated children molecules from their parent molecule and assigned them a consecutive ID number to each new children, keeping all those data in memory to avoid repetitions. Each of the 3 consecutive runs randomly re-starts the initial parent for a unique co-evolution pathway. **Blue**, targeting children < 300 g/mol. **Green**, targeting children < 400 g/mol. **Red**, targeting children < 600 g/mol.

Table S3

F13L-1, F13L0, F13L1 and F13L2 amino acids around 4 Å of ADV docked top-children

Amino acids	F13L0-ST246	F13L1-ST246	12326	8181	F13L2-ST246	35702	34853
52	F	Phe					
53	C	Cys					
55	N	Asn					
58	S	Ser	H				
86	A	Ala					
89	R	Arg					
116	L	Leu					
118	L	Leu					
120	C	Cys					
133	N	Asn					
135	S	Ser	H	H		H	H
137	T	Thr		H			
139	G	Gly					
140	S	Ser					
144	I	Ile					
239	L	Leu					
246	R	Arg				H	H
267	N	Asn			267		
279	W	Trp					
*280	D	Asp					
281	K	Lys	H		H		
282	N	Asn					
*283	D	Asp				H	
284							
311							
*312	N	Asn					H
*314	K	Lys	H				
326	S	Ser					
327	S	Ser		H			
328	N	Asn			H		
329	N	Asn				H	H
331	D	Asp					
333	T	Thr					
*334	H	His		H			H
*338	H	His					H

Amino acid positions, were those at F13L0, except the <sup>267</sup>N which was either mutated to D or deleted (▼). For comparative purposes, the numbers > 267 of F13L2 <sup>267</sup>N deleted mutations were corrected to their initial positions in F13L0 and F13L1.

\*red number, F13L amino acid of resistant vaccinia mutation to ST246 and IMCBH<sup>24</sup>.

\*green numbers, F13L mapping of conserved amino acids at the near-canonical phospholipase-like motif in poxviruses and Histidines possibly participating in their phospholipase activity. **Blue** and **yellow** rectangle backgrounds, residues of F13L1 and F13L2 predicted at 4 Å to reference ligand and top-children atoms (LigPlus/LigPlot).

**Yellow background numbers to the left**, F13L amino acids previously identified by ST246 docking in the MPXV strain of 2007 (<sup>35E</sup>).

**H**, LigPlus/LigPlot predicted Hydrogen bonds.

## Funding

The work was carried out without any external financial contribution

## Competing interests

The author declares no competing interests

## Authors' contributions

JC designed, performed and analyzed the dockings and drafted the manuscript.

## Acknowledgements

Thanks are due to Dra.M.Lorenzo and Dr.R.Blasco at CSIC-INIA Dpt.Biotecnologia Madrid (Spain) for their initial idea and critical reading of a previous version of this manuscript. Thanks are specially due to Dr. T.Sander, J.Wahl and N.Berndt of Idorsia Pharmaceuticals Ltd. at Allschwil (Switzerland) for their help with the Windows version of the Data Warrior Build Evolutionary Library, files to solve initial memory problems, and the inclusion of Toxicity risks assessment into the DW-BEL algorithms. Special thanks to N.Berndt for his original discussions and help with the Toxicity - Nastic and 2D geometry conservation macro designs. Thanks are also due to Joshua Holliday of the PCSPECIALIST support team at Wakefield WF4 4TD England, for his help with the design and duplication of our computer RAM memories. Thanks also to Dr. A. Villena from the University of Leon (Spain) for maintaining a permanent flow of recent bibliography.

## References

- Coll, J.M. Exploring non-toxic co-evolutionary docking. *ChemRxiv*. 2023. <https://chemrxiv.org/engage/chemrxiv/article-details/6512b162ade1178b2424c325> <http://dx.doi.org/10.26434/chemrxiv-2023-r5b0>.
- Husain, M. and Moss, B. Vaccinia virus F13L protein with a conserved phospholipase catalytic motif induces colocalization of the B5R envelope glycoprotein in post-Golgi vesicles. *J Virol*. 2001, 75: 7528-42 <http://dx.doi.org/10.1128/JVI.75.16.7528-7542.2001>.
- Husain, M., et al. Topology of epitope-tagged F13L protein, a major membrane component of extracellular vaccinia virions. *Virology*. 2003, 308: 233-42 [http://dx.doi.org/10.1016/S0042-6822\(03\)00663-1](http://dx.doi.org/10.1016/S0042-6822(03)00663-1).
- Leiros, I., et al. The reaction mechanism of phospholipase D from *Streptomyces sp.* strain PMF. Snapshots along the reaction pathway reveal a pentacoordinate reaction intermediate and an unexpected final product. *J Mol Biol*. 2004, 339: 805-20 <http://dx.doi.org/10.1016/j.jmb.2004.04.003>.
- Bryk, P., et al. Vaccinia Virus Phospholipase Protein F13 Promotes Rapid Entry of Extracellular Virions into Cells. *J Virol*. 2018, 92: <http://dx.doi.org/10.1128/JVI.02154-17>.
- Koonin, E.V. A duplicated catalytic motif in a new superfamily of phosphohydrolases and phospholipid synthases that includes poxvirus envelope proteins. *Trends Biochem Sci*. 1996, 21: 242-3 [http://dx.doi.org/S0968-0004\(96\)30024-8](http://dx.doi.org/S0968-0004(96)30024-8) [pii].
- Ponting, C.P. and Kerr, I.D. A novel family of phospholipase D homologues that includes phospholipid synthases and putative endonucleases: identification of duplicate repeats and potential active site residues. *Protein Sci*. 1996, 5: 914-22 <http://dx.doi.org/10.1002/pro.550050513>.
- Chen, Y., et al. Vaccinia virus p37 interacts with host proteins associated with LE-derived transport vesicle biogenesis. *Virology*. 2009, 6: 44 <http://dx.doi.org/10.1186/1743-422X-6-44>.
- Blasco, R. and Moss, B. Extracellular vaccinia virus formation and cell-to-cell virus transmission are prevented by deletion of the gene encoding the 37,000-Dalton outer envelope protein. *Journal Virology*. 1991, 65: 5910-5920.
- Schmutz, C., et al. A mutation in the gene encoding the vaccinia virus 37,000-Mr protein confers resistance to an inhibitor of virus envelopment. *J Virol*. 1991, 65: 3435-42 <http://dx.doi.org/10.1128/JVI.65.7.3435-3442.1991>.
- Tan, C., et al. Development of multi-epitope vaccines against the monkeypox virus based on envelope proteins using immunoinformatics approaches. *Front Immunol*. 2023, 14: 1112816 <http://dx.doi.org/10.3389/fimmu.2023.1112816>.
- Lorenzo, M.M., et al. Mutagenesis of the palmitoylation site in vaccinia virus envelope glycoprotein B5. *J Gen Virol*. 2012, 93: 733-743 <http://dx.doi.org/10.1099/vir.0.039016-0>.
- Perdigueru, B. and Blasco, R. Interaction between vaccinia virus extracellular virus envelope A33 and B5 glycoproteins. *J Virol*. 2006, 80: 8763-77 <http://dx.doi.org/10.1128/JVI.00598-06>.
- Isaacs, S.N., et al. Characterization of a vaccinia virus-encoded 42-kilodalton class I membrane glycoprotein component of the extracellular virus envelope. *J Virol*. 1992, 66: 7217-24 <http://dx.doi.org/10.1128/JVI.66.12.7217-7224.1992>.
- Engelstad, M. and Smith, G.L. The vaccinia virus 42-kDa envelope protein is required for the envelopment and egress of extracellular virus and for virus virulence. *Virology*. 1993, 194: 627-37 <http://dx.doi.org/10.1006/viro.1993.1302>.
- Howechurch, K.M., et al. The vaccinia virus F13L YPPL motif is required for efficient release of extracellular enveloped virus. *J Virol*. 2007, 81: 7310-5 <http://dx.doi.org/10.1128/JVI.00034-07>.
- Ali, Y., et al. Fragment-Based Approaches Identified Tecovirimat-Competitive Novel Drug Candidate for Targeting the F13 Protein of the Monkeypox Virus. *Viruses*. 2023, 15: <http://dx.doi.org/10.3390/v15020570>.
- Wang, J., et al. An Overview of Antivirals against Monkeypox Virus and Other Orthopoxviruses. *J Med Chem*. 2023, 66: 4468-4490 <http://dx.doi.org/10.1021/acs.jmedchem.3c00069>.
- DeLaurentis, C.E., et al. New Perspectives on Antimicrobial Agents: Tecovirimat for Treatment of Human Monkeypox Virus. *Antimicrob Agents Chemother*. 2022, 66: e0122622 <http://dx.doi.org/10.1128/aac.01226-22>.
- Frenois-Veyrat, G., et al. Tecovirimat is effective against human monkeypox virus in vitro at nanomolar concentrations. *Nat Microbiol*. 2022, 7: 1951-1955 <http://dx.doi.org/10.1038/s41564-022-01269-8>.
- Duraifour, S., et al. Specific targeting of the F13L protein by ST-246 affects orthopoxvirus production differently. *Antivir Ther*. 2008, 13: 977-90.
- Gaada, M.M., et al. Movements of vaccinia virus intracellular enveloped virions with GFP tagged to the F13L envelope protein. *J Gen Virol*. 2001, 82: 2747-2760 <http://dx.doi.org/10.1099/0022-1317-82-11-2747>.
- Lam, H.Y., et al. In Silico Repurposed Drugs against Monkeypox Virus. *Molecules*. 2022, 27: <http://dx.doi.org/10.3390/molecules27165277>.
- Duraifour, S., et al. ST-246 is a key antiviral to inhibit the viral F13L phospholipase, one of the essential proteins for orthopoxvirus wrapping. *J Antimicrob Chemother*. 2015, 70: 1367-80 <http://dx.doi.org/10.1093/ac/cku545>.
- Li, D., et al. Targeting F13 from monkeypox virus and variola virus by tecovirimat: Molecular simulation analysis. *J Infect*. 2022, 85: e99-e101 <http://dx.doi.org/10.1016/j.jinf.2022.07.001>.
- Bojkova, D., et al. Drug Sensitivity of Currently Circulating Mpox Viruses. *N Engl J Med*. 2023, 388: 279-281 <http://dx.doi.org/10.1056/NEJM.22.21336>.
- Garrigues, J.M., et al. Identification of Tecovirimat Resistance-Associated Mutations in Human Monkeypox Virus - Los Angeles County. *Antimicrob Agents Chemother*. 2023, 67: e0056823 <http://dx.doi.org/10.1128/aac.00568-23>.
- Smith, T.G., et al. Tecovirimat Resistance in Mpox Patients, United States, 2022-2023. *Emerg Infect Dis*. 2023, 29: <http://dx.doi.org/10.3201/e2912.231146>.
- Milja, O., et al. Mpox in people with advanced HIV infection: a global case series. *Lancet*. 2023, 401: 939-949 [http://dx.doi.org/10.1016/S0140-6736\(23\)02733-8](http://dx.doi.org/10.1016/S0140-6736(23)02733-8).
- Kato, N., et al. Inhibition of release of vaccinia virus by N1-isonicotinyl-N2-3-methyl-4-chlorobenzoylhydrazine. *J Exp Med*. 1969, 129: 795-808 <http://dx.doi.org/10.1084/jem.129.4.795>.
- Coll, J.M. Evolutionary-docking targeting bacterial FtsZ. *ChemRxiv*. 2023. <https://chemrxiv.org/engage/chemrxiv/article-details/6405c36cc600523a3bc6b79> <http://dx.doi.org/10.26434/chemrxiv-2023-l9d93>.
- Wahl, J., et al. Accuracy evaluation and addition of improved dihedral parameters for the MMFF94s. *J Cheminform*. 2019, 11: 53 <http://dx.doi.org/10.1186/s13321-019-3371-8>.
- Coll, J. Could Acinetobacter baumannii L6-abacouin docking be improved? *ChemRxiv*. 2023. <https://chemrxiv.org/engage/chemrxiv/article-details/649aa71aba3e9daef1d1756> <http://dx.doi.org/10.26434/chemrxiv-2023-962h>.
- Bryant, P., et al. Structure prediction of protein-ligand complexes from sequence information with Umlol. *bioRxiv*. 2023: <http://dx.doi.org/10.1101/2023.11.03.565471>.
- Coll, J. Star-shaped Triazine-derivatives: would they crossbind SARS-CoV-2 spike helices? *ChemRxiv*. 2021. <https://chemrxiv.org/engage/chemrxiv/article-details/6133c1096563696d9d22bbd> <http://dx.doi.org/10.33774/chemrxiv-2021-r68xv-2>.
- Lorenzo, M.M., et al. Would it be possible to stabilize prefusion SARS-CoV-2 spikes with ligands? *ChemRxiv*. 2021: <http://dx.doi.org/10.26434/chemrxiv.13453919-2>.
- Bermejo-Nogales, A., et al. Computational ligands to VKORCs and CYPs. Could they predict new anticouagulant rodenticides? *BioRxiv*. 2021: <http://dx.doi.org/10.1101/2021.01.22.426921>.
- Dallakyan, S. and Olson, A.J. Small-molecule library screening by docking with PyRx. *Methods Mol Biol*. 2015, 1263: 243-50 [http://dx.doi.org/10.1007/978-1-4939-2268-7\\_19](http://dx.doi.org/10.1007/978-1-4939-2268-7_19).
- Morris, G.M., et al. AutoDock4 and AutoDockTools4: Automated docking with selective receptor flexibility. *J Comput Chem*. 2009, 30: 2785-91 <http://dx.doi.org/10.1002/jcc.2125>.
- Huey, R., et al. A semiempirical free energy force field with charge-based desolvation. *J Comput Chem*. 2007, 28: 1145-52 <http://dx.doi.org/10.1002/jcc.20634>.
- Trott, O. and Olson, A.J. AutoDock Vina: improving the speed and accuracy of docking with a new scoring function, efficient optimization, and multithreading. *J Comput Chem*. 2010, 31: 455-61 <http://dx.doi.org/10.1002/jcc.21334>.
- Yang, G., et al. An orally bioavailable antipoxvirus compound (ST-246) inhibits extracellular virus formation and protects mice from lethal orthopoxvirus challenge. *J Virol*. 2005, 79: 13139-49 <http://dx.doi.org/10.1128/JVI.79.20.13139-13149.2005>.
- Fernuz, N., et al. ProtFP12 is a deep unsupervised language model for protein design. *Nat Commun*. 2022, 13: 4348 <http://dx.doi.org/10.1038/s41467-022-30027-0>.
- Fernuz, N. and Hooker, B. Dreaming ideal protein structures. *Nat Biotechnol*. 2022, 40: 171-172 <http://dx.doi.org/10.1038/s41587-021-01196-9>.
- Fernuz, N., et al. From sequence to function through structure: Deep learning for protein design. *Comput Struct Biotechnol J*. 2023, 21: 238-250 <http://dx.doi.org/10.1016/j.csbj.2022.11.014>.
- Grechshnikova, D. Transformer neural network for protein-specific drug generation as a machine translation problem. *Sci Rep*. 2021, 11: 321 <http://dx.doi.org/10.1038/s41598-020-79892-4>.
- Ivanenkov, Y.A., et al. Chemistry42: An AI-Driven Platform for Molecular Design and Optimization. *J Chem Inf Model*. 2023, 63: 695-701 <http://dx.doi.org/10.1021/acs.jcim.2c01191>.
- Kang, K.M., et al. AI-based prediction of new binding site and virtual screening for the discovery of novel P2X3 receptor antagonists. *Eur J Med Chem*. 2022, 240: 114556 <http://dx.doi.org/10.1016/j.ejmech.2022.114556>.
- Mock, M., et al. AI can help to speed up drug discovery - but only if we give it the right data. *Nature*. 2023, 621: 467-470 <http://dx.doi.org/10.1038/d41586-023-02896-9>.
- Tsaban, T., et al. Harnessing protein folding neural networks for peptide-protein docking. *Nat Commun*. 2022, 13: 176 <http://dx.doi.org/10.1038/s41467-021-27838-8>.